Prediction of Survival with Fluorine-18-Fluorodeoxyglucose and PET in Head and Neck Cancer

Heikki Minn, Maria Lapela, Pekka J. Klemi, Reidar Grénman, Sirkku Leskinen, Paula Lindholm, Jörgen Bergman, Esa Eronen, Merja Haaparanta and Heikki Joensuu

Departments of Oncology and Radiotherapy, Pathology, Otorhinolaryngology, Cyclotron-PET Center, University of Turku, Turku; and Department of Oncology, University of Helsinki, Helsinki, Finland

The aim of this prospective study was to investigate if high uptake of ^{18}F-fluoro-2-deoxy-D-glucose (FDG) is associated with aggressiveness in head and neck cancer and low probability of survival. **Methods:** Thirty-seven patients with squamous-cell carcinoma of the head and neck underwent FDG-PET in the fasting state before cancer treatment. FDG uptake in primary tumor was quantitated as the standardized uptake value of FDG normalized to the predicted lean body mass (SUV_{lean}, n = 37) and as the graphically determined metabolic rate for FDG (rMR_{FDG}, n = 34). Paraffin-embedded tumor samples were used for histologic evaluation, and expression of cytokeratin and Ki-67 antigen were assessed by immunohistochemistry. **Results:** Interobserver agreement for the determination of quantitative uptake of FDG in tumors was excellent ($r^2 = 0.996$, p < 0.00001), and all 37 primary tumors were visualized. A high uptake of FDG as assessed by SUV_{lean} was associated with a higher than the median mitotic count (p = 0.01), absence of keratinization (p = 0.03), low or moderate histological grade of differentiation (p = 0.046) and advanced stage (p = 0.03), but not with Ki-67 expression (p = 0.11). The overall survival of patients with a SUV_{lean} lower than or equal to the median value (9.0) was clearly better in univariate analysis than that of patients with a SUV_{lean} higher than the median (3-yr survival 73% versus 22%, relative risk of death (RR) 4.2, 1.6–11.0). However, in a multivariate analysis the only independent predictors of survival were the mitotic count (RR 4.0, 1.4–11.7) and stage (3.8, 1.2–12.2). **Conclusion:** High uptake of FDG in untreated head and neck cancer is associated with advanced disease, and may portend poor survival. Aggressive treatment approaches should be considered for patients presenting with a tumor with high uptake of FDG.

Key Words: head neoplasms; neck neoplasms; tumor grading; survival; PET

Squamous-cell carcinoma of the head and neck is a histologically distinct yet clinically heterogenous entity with a variable response to treatment. Standard primary therapy consists of radiotherapy and/or surgery, and more advanced cases are sometimes treated with chemotherapy in a concomitant or neoadjuvant setting (1,2). The unpredictable clinical behavior of head and neck squamous-cell carcinoma and the recognition of the significance of several radiobiologically relevant tumor-related parameters, e.g., proliferation (3), growth factor expression (4) and vascularization (5), have prompted an intensive search for clinically measurable biological factors that would assist in selection of optimal treatment and evaluation of prognosis.

PET imaging with ^{18}F-fluoro-2-deoxy-D-glucose (FDG) is comparable to CT and MRI in detection of both primary tumors and lymph node metastases of head and neck squamous-cell

carcinoma (6–8). Furthermore, FDG uptake has been proposed to be linked to malignant potential of head and neck squamous-cell carcinoma (9) in accordance with studies on gliomas (10), soft-tissue sarcomas (11) and non-Hodgkin lymphomas (12), where increased FDG uptake has been associated with a high-grade tumor. This study was designed to assess characterization of the malignancy of head and neck squamous-cell carcinoma with PET by comparing FDG uptake in primary tumor with several established prognostic factors during the initial diagnostic work-up. Both uni- and multivariate analyses were performed to assess whether FDG uptake is associated with survival.

MATERIALS AND METHODS

Patients and Treatment

Between January 1991 and September 1994, 37 patients with newly diagnosed head and neck squamous-cell carcinoma underwent an FDG-PET study before treatment. Nondiabetic patients with a WHO performance status ranging from 0–2 and a histologically verified primary head and neck squamous-cell carcinoma were eligible. Only tumors with a minimum diameter of 2 cm were included in the study. Routine blood chemistry including hemoglobin concentration was obtained in each case. All patients had panendoscopy and CT scans of the primary tumor site and the neck and were staged according to the guidelines proposed by the International Union Against Cancer (13). CT scanning and clinical inspection were used to calculate primary tumor volumes in three perpendicular directions, as described previously (14). The study protocol was reviewed and approved by the Ethics Committee of Turku University Central Hospital. Written consent was obtained for each patient.

All patients were treated after PET imaging with a curative intent; characteristics are listed in Table 1. Sixteen patients had definitive radiotherapy to a total dose of 64–72 Gy, 19 patients underwent preoperative radiotherapy of 60–65 Gy and two patients had surgery followed by radiation to 60 Gy. The fractionation schedule was standard in all but two patients (2.0 Gy per fraction, 5 fractions a week). Two patients underwent a preoperative accelerated hyperfractionated radiation regimen (1.6 Gy b.i.d) to 64 Gy in 5 wk. Four patients did not receive the prescribed radiation dose because of marked clinical deterioration during treatment. Primary tumor was radically resected in 19 patients, and 13 patients had either radical (n = 3), functional (n = 5) or supraomohyoidal (n = 5) neck dissection. After radiotherapy and surgery, patients were followed up at 3-mo intervals; median follow-up time was 43 mo (range, 10–53 mo).

PET Imaging

PET studies were performed in the fasting state, and the mean ± s.d. plasma glucose and insulin concentrations during the study were 5.5 ± 0.6 mmol/l (n = 37) and 12 ± 12 mU/l (n = 33), respectively. PET imaging was performed with a Siemens ECAT

TABLE 1
Patient and Tumor Characteristics

		No. of patients	Percent (%)
Gender	Male	26	70
	Female	11	30
Age (yr)	>65	22	59
	≤65	15	41
WHO performance status	0	9	24
	1	18	49
	2	10	27
Blood hemoglobin (g/liter)	≤12.0	7	19
	12.1–13.0	8	22
	13.1–14.0	14	38
	≥14.1	8	22
Site of primary tumor	Oral cavity	15	40
	Oropharynx	1	3
	Nasopharynx	5	11
	Hypopharynx	5	14
	Larynx	10	27
	Parotid gland	2	5
Primary tumor size	T1	1	3
	T2	10	27
	T3	12	32
	T4	14	38
Nodal status	N0	18	49
	N1	10	27
	N2	9	24
UICC stage	II	7	19
	III	10	27
	IV	20	54
Histological grade of differentiation	G1	12	32
	G2	20	54
	G3	5	14

WHO = World Health Organization; UICC = International Union Against Cancer.

931/08 (Knoxville, TN) positron scanner. FDG was synthesized with an automatic apparatus by a previously described nucleophilic substitution procedure (15), and patients received 296 ± 18 MBq as an intravenous bolus injection after being positioned supine on the couch with the tumor in the field of view. Attenuation correction was measured in all patients with a preinjection transmission scan using a ring-source filled with ^{68}Ga/^{68}Ge. The acquisition time was 60 min starting immediately after FDG injection in 33 patients (dynamic mode; a total of 20 frames) and 20 min in four patients whose tumor imaging started 45 min after the injection (steady-state mode; a total of four frames). The details of the dynamic imaging procedure and the sequence of the associated blood sampling are described elsewhere (16).

Quantitation of FDG Uptake

Sinogram data were corrected for dead time, decay and photon attenuation and reconstructed in a 256 × 256 matrix using a Hann-filter with a cutoff frequency of 0.5. The final x-y resolution after these procedures was 8-mm FWHM in-plane. In all 37 patients, the primary head and neck squamous-cell carcinoma was detectable as an area of increased FDG uptake in a scan obtained between 55 and 60 min from injection. This scan was used for quantification of FDG uptake by using a semiautomated algorithm for defining a region of interest (ROI) in a tumor with maximum uptake (17,18). The algorithm determines average counting rate per voxel in a rectangular ROI of predetermined size having the highest radioactivity within a large, investigator-defined ROI comprising the whole tumor. The volume of this maximum ROI was fixed at 0.2 ± 0.05 cm^3. To evaluate interobserver variability

in judgement of FDG uptake, a manually determined second ROI in tumor was defined by another investigator blinded both to clinical data and the results of the semiautomatic analysis. Subsequently, an FDG uptake index was assessed in the steady-state mode by using the formula for calculation of the standardized uptake value adjusted to the predicted value of lean body mass (SUV$_{lean}$) (17) as follows:

$$SUV_{lean} = \frac{\text{Radioactivity concentration in ROI (Bq/ml)}}{\text{Injected dose (Bq)/lean body mass (g)}} . \quad \text{Eq. 1}$$

In patients imaged according to the dynamic protocol (n = 33), an FDG influx constant (K$_i$) was determined by graphical analysis (12,16,18). K$_i$ describes the net phosphorylation rate of FDG per unit time and gives, when multiplied by plasma glucose concentration during PET study, the metabolic rate for FDG (K$_i$ × plasma glucose concentration = rMR$_{FDG}$) (16,18). SUV$_{lean}$ is a dimensionless parameter, and the unit for rMR$_{FDG}$ is μmol/100 g/min. To avoid confusion with true glucose metabolic rates, a nomenclature referring to regional metabolic rates for FDG in tumor (i.e., rMR$_{FDG}$) was applied.

Histologic Evaluation

The paraffin-embedded 4 μm-thick tissue sections were stained with hematoxylin and eosin for histopathologic diagnosis, counting of mitotic figures per square mm of (volume corrected) tumor tissue, and for scoring histological grade of differentiation and the degree of keratinization using WHO criteria (5). The number of mitotic figures was calculated from areas of well-preserved cancer with 8–13 fields per tumor. The degree of keratinization was scored as follows: 0 = no keratinization, 1 = individual cell keratinization and some keratin pearls and 2 = heavy keratinization and many keratin pearls.

Parallel sections were immunostained with the rabbit primary anti human Ki-67 antigen (DAKO, Copenhagen, Denmark) for detecting proliferating cells according to the method described earlier (19). The specimen was first assessed from several low power fields, then the percentage of Ki-67 positive cells in the areas containing well-preserved cancer without keratinization were semiquantitatively assessed by using a 40 × objective and an ocular with a rectangle of a microscope (Leitz, Dialux 22, Viereich, Germany). All histologic evaluation was assessed from numerically coded slides without any knowledge of survival, PET or other clinical data.

Statistical Analysis

Statistical analysis was performed with a BMDP-computer program (BMDP Statistical Software, Inc., Los Angeles, CA). Relationships between the semiautomatically computed and manually determined tumor ROIs and SUV$_{lean}$ versus rMR$_{FDG}$ were assessed by linear regression. Survival times were calculated from the time of the PET study, which was performed 18 ± 14 days before start of treatment (range 0–42 days). The cumulative survival was estimated with the product-limit method and comparison of the cumulative survival between groups was made with the log-rank test. The relative importance of prognostic factors was analyzed using Cox's proportional hazard model. Frequency distribution tables were calculated with the chi-square or Fisher's exact test. All p values are two-tailed.

RESULTS

In a blinded visual evaluation of PET scans, all but one were correctly identified. The only misinterpretation was of normal mucosal activity in the vicinity of a T2-tumor in buccal mucosa. This primary tumor could also be visualized when clinical data were made available to the interpreter. The subsequent calculation of FDG uptake, based on this blinded analysis and the

determination of maximum uptake with computed algorithm, resulted in an excellent agreement between the SUV_{lean}s obtained from visual and semiquantitative analyses ($r^2 = 0.996$, $p < 0.00001$).

The median SUV_{lean} for well-differentiated tumors was 7.9 (range 2.7–14.7, n = 12), for moderately differentiated tumors 8.8 (range 3.5–16.6, n = 20), and for poorly differentiated tumors 11.3 (range 10.5–13.5, n = 5). The median rMR_{FDG}s were 25.3 μmol/100 g/min (range 13.9–46.0 μmol/100 g/min, n = 10), 25.4 μmol/100 g/min (range 9.5–59.1 μmol/100 g/min, n = 18) and 40.9 μmol/100 g/min (range 28.1–51.5 μmol/100 g/min, n = 5) for well, moderately and poorly differentiated tumors, respectively. Both of the two salivary gland tumors had a relatively low tracer uptake: a well-differentiated parotid carcinoma had a SUV_{lean} of 6.0 and a moderately differentiated carcinoma 4.0, respectively. The correlation between FDG uptake calculated in the steady state (SUV_{lean}) and dynamic modes (rMR_{FDG}) was high ($r^2 = 0.84$, $p < 0.0001$, n = 33). There was no obvious correlation between tumor volume and FDG uptake, although larger tumors tended to show higher rMR_{FDG} than tumors with a volume < 10 cm^3 (Fig. 1). Representative FDG-PET scans of head and neck squamous-cell carcinoma with high and low FDG uptake are shown in Figure 2. This figure illustrates that both tumors are readily discernible against the background of lower ^{18}F activity in neck tissues and oral mucosa after 55–60 min from injection.

The median values for all SUV_{lean} s (n = 37) and rMR_{FDG}s (n = 33) are given in Table 2, which shows the association of nine clinicopathologic factors with the FDG uptake in tumor. A higher than median uptake of FDG, expressed as SUV_{lean}, was associated with an advanced disease stage (p = 0.03), a low or moderate histological grade of differentiation (p = 0.046), higher than the median number of mitoses (p = 0.01) and the lack of keratinization (p = 0.03) was also seen. Of these, only the degree of tumor keratinization (p = 0.02) was significantly associated with higher than the median rMR_{FDG}, although the relationship between a high rMR_{FDG} and a high mitotic count was almost significant (p = 0.06). Ki-67 expression was not related to either of the two FDG uptake indexes.

In a univariate survival analysis, significant difference in survival was seen between patients with tumors with a SUV_{lean} larger or smaller than the median (p = 0.002, relative risk of dealth (RR) 4.2, 95% confidence interval, 1.6–11.0, Fig. 3). The same trend was seen for rMR_{FDG}, with an almost significant difference in outcome (p = 0.07, RR 2.4, 95% confidence interval, 0.9–6.1). Of the nine factors listed in Table 2, the parameters associated with poor prognosis were the presence of higher than the median number of mitoses per square mm (p = 0.001, RR 4.9, 95% confidence interval, 1.8–13.0) and advanced disease stage (p = 0.01, RR 3.3, 95% confidence interval, 1.3–8.8). When SUV_{lean} and rMR_{FDG} were entered into a multivariate analysis together with these other two factors, only the number of mitoses (p = 0.004, RR 4.0, 95% confidence interval, 1.4–11.7) and the International Union Against Cancer (UICC) stage (p = 0.02, RR 3.8, 95% confidence interval, 1.2–22.2) had independent influence on survival. The two FDG uptake indexes, SUV_{lean} and rMR_{FDG}, were both associated with the mitotic count (Table 2) and did not, therefore, have independent prognostic significance in a multivariate analysis.

DISCUSSION

In vivo imaging of human tumors with FDG-PET is a clinical extension of classical studies on carbohydrate metabolism, which demonstrated that a high rate of glycolysis is one of the
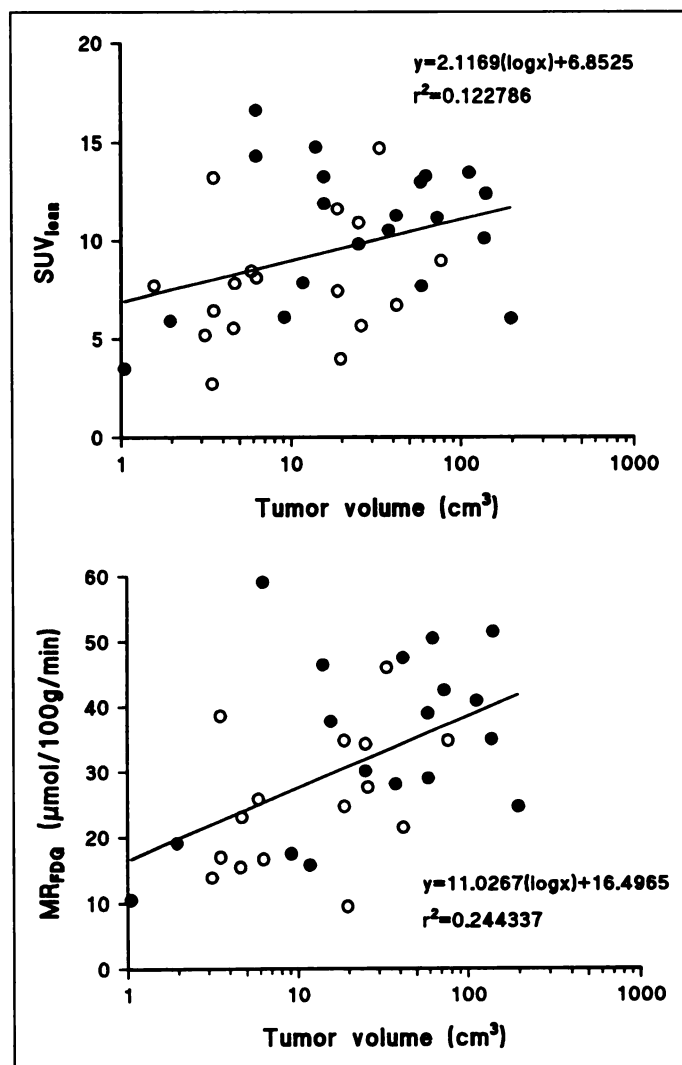
FIGURE 1. Comparison of tumor volume with FDG uptake (SUV_{lean}, n = 37; rMR_{FDG}, n = 33) in head and neck cancer. Open circles represent tumors of patients alive after median follow-up time of 43 mo since the PET study; solid circles represent tumors of patients who have died during follow-up.

most conspicuous characteristics of the cancer cell phenotype (20). This preference for nonoxidative catabolism of glucose has been associated with increased hexose transport (21) and
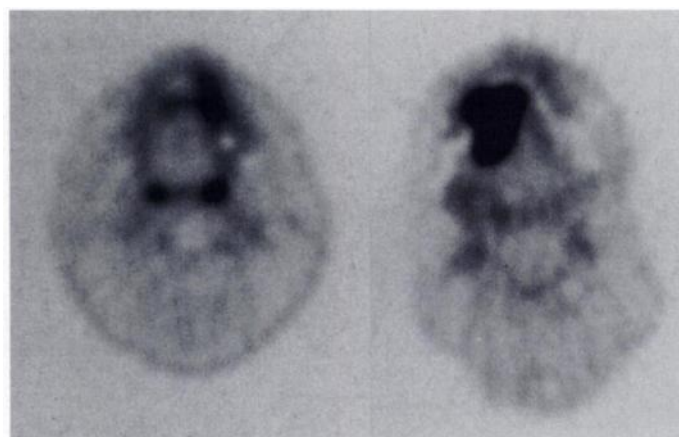
FIGURE 2. FDG-PET images of patients with head and neck cancers. (Left) A well differentiated squamous-cell carcinoma in maxillary gingiva with SUV_{lean} = 5.2. (Right) A moderately differentiated squamous-cell carcinoma in mandibular gingiva with SUV_{lean} = 9.8. Dorsal of the left tumor with lower FDG uptake, normal tissue uptake of tracer is seen bilaterally in the palatine tonsils.

TABLE 2
Association of Nine Factors with FDG Uptake in Head and Neck Cancer

Variable/class		FDG uptake					
		Steady-state mode (n = 37)			Dynamic mode (n = 33)		
		SUV$_{lean}$ ≤9.0* n (%)	SUV$_{lean}$ >9.0 n (%)	p-value	SUV$_{lean}$ ≤29.0† n (%)	SUV$_{lean}$ >29.0 n (%)	p-value
Gender	Male	13 (50)	13 (50)	0.80	11 (46)	13 (54)	0.44
	Female	6 (55)	5 (45)		6 (67)	3 (33)	
Performance staus (WHO)	0 or 1	15 (56)	12 (44)	0.48	13 (57)	10 (43)	0.46
	2	4 (40)	6 (60)		4 (40)	6 (60)	
Age (yr)	≤68*	10 (53)	9 (47)	0.87	10 (53)	9 (47)	0.88
	>68	9 (50)	9 (50)		7 (50)	7 (50)	
Blood hemoglobin (g/dl)	≤13.4*	12 (60)	8 (40)	0.25	10 (56)	8 (44)	0.61
	>13.4	7 (41)	10 (59)		7 (47)	8 (53)	
UICC stage	II or III	12 (71)	5 (29)	0.03	9 (69)	4 (31)	0.10
	IV	7 (35)	13 (65)		8 (40)	12 (60)	
Histological grade	G1	9 (75)	3 (25)	0.05	7 (70)	3 (30)	0.16
	G2 or G3	10 (40)	15 (60)		10 (44)	13 (57)	
Number of mitoses (/mm²)	≤0.4*	14 (70)	6 (30)	0.01	12 (67)	6 (33)	0.06
	>0.4	5 (29)	12 (71)		5 (33)	10 (67)	
Degree of keratinization	1 or 2	13 (68)	6 (32)	0.03	11 (73)	4 (27)	0.02
	0	6 (33)	12 (67)		6 (33)	12 (67)	
Ki-67 expression (%)	≤40*	11 (61)	7 (39)	0.11	9 (56)	7 (44)	0.37
	<40	3 (30)	7 (70)		3 (38)	5 (63)	

*Median value.
†The unit for MR$_{FDG}$ is $\mu mol/100g/min$.
WHO = World Health Organization; UICC = International Union Against Cancer

tumor growth rate (22) in a manner which could logically be exploited for malignancy grading with PET. The study results are especially useful in head and neck squamous-cell carcinoma where surgical treatment and radiotherapy are often combined, and the use of unconventional fractionation schedules and chemotherapy may improve outcome if individual tumor characteristics are accounted for (1,3).

The association of high FDG uptake with poor survival may be related to several factors. Most importantly, patients with advanced disease present with large tumors, and FDG uptake reflects simply the large tumor burden and associated co-morbid conditions in these patients. We hypothesize that abnormalities in host carbohydrate metabolism seen in the cachectic state are responsible for an unbalanced glucose flux between the neoplastic and peripheral tissues, contributing to

FIGURE 3. FDG uptake, expressed as SUV$_{lean}$ in relation to survival in 37 patients with head and neck squamous-cell carcinoma. The percentages refer to the 3-yr survival.

increased FDG uptake in tumors of patients with advanced malignancies (23). Our study included mostly patients with advanced disease (81% had UICC Stage III to IV) and, although influence of partial volume effects could potentially lead to underestimation of FDG uptake in early primary lesions, our findings do not support a relationship between absolute tumor volume and tracer accumulation. It is possible, however, that correction for count recovery in small lesions would improve grading of tumors based on metabolic activity.

In this study, an association between FDG uptake and the number of mitoses was demonstrated. This is in agreement with previous experience, where imaging of head and neck tumors with FDG by a modified gamma camera or PET has been compared to the cellular proliferative activity, as evaluated by DNA flow cytometry (9,24). The presence of similar relationship in nonepithelial malignancies such as non-Hodgkin's lymphoma (12) and musculoskeletal soft tissue tumors (11) provides further evidence that the rate of tumor glucose metabolism may be a meaningful marker of malignancy in the clinical setting. Although FDG uptake in head and neck squamous-cell carcinoma and other tumors may also be evaluated in a simple qualitative fashion (6), this study lends support to quantitative uptake measurements, which confer additional information not available with other tomographic imaging modalities. A short scan between 45–60 min after injection of FDG is usually appropriate for clinical purposes (16). We emphasize, however, that the influence of host metabolic and nutritional status on FDG uptake in tumor requires adherence to fasting conditions and corrections for tissue compartments with a low affinity for FDG (16,17). Another matter of concern for the use of a sugar analog is the heterogeneity of neoplastic tissues, which precludes direct calculations of the true glucose metabolic rates for tumors on the basis of FDG uptake (25).

Our study suggests that high FDG uptake in head and neck squamous-cell carcinoma is linked to established markers of poor outcome such as advanced stage, lack of keratinization and high number of mitoses. Although FDG uptake did not show
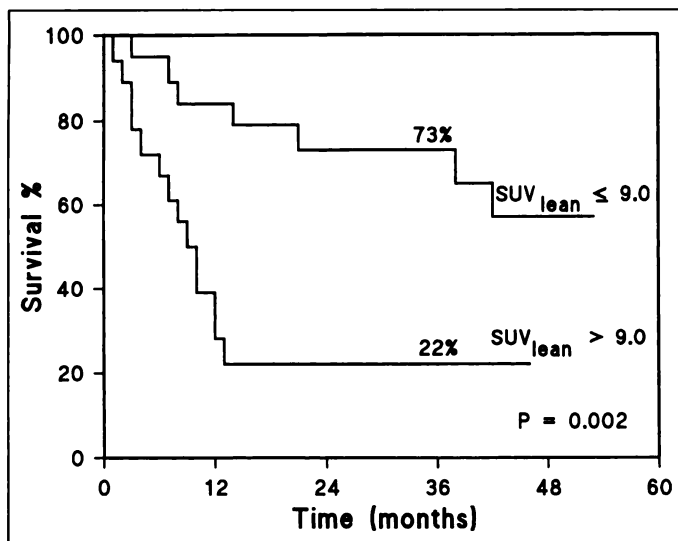
independent prognostic significance in multivariate analysis, quantitative FDG-PET is a viable adjunct to conventional clinical and histologic assessment due to the noninvasive nature of the procedure, good reproducibility and complete freedom from sampling errors (*18*). The method provides an opportunity to simultaneous evaluation of the lymphatic spread and later monitoring of treatment, clearly complementing morphologic imaging with CT or MRI (*6–8,26*). Improvements in the technique include correction for loss of count recovery in small tumors and use of high-resolution PET scanners, which enable better discrimination of the most aggressive parts of the tumor in a three-dimensional display. It would be important to compare FDG uptake in tumors and perhaps lymph node metastases of less than 2 cm in diameter to study how well malignant behavior may be assessed in head and neck squamous-cell carcinoma of early stage. Although theoretically dynamic methods with blood sampling improve time-independency in quantitative assessment of FDG uptake, it is still debatable whether they should replace shorter acquisition protocols in routine clinical practice.

CONCLUSION

FDG-PET is useful for evaluation of malignancy grade of primary head and neck squamous-cell carcinoma. Patients presenting with a tumor with high FDG accumulation have a risk for poor survival and should be considered for intensive treatment protocols including hyperfractionated radiotherapy and/or chemotherapy. The advantage of using FDG-PET for evaluation of aggressiveness of cancer is the noninvasive nature of the procedure and the potential to simultaneously assist in tumor localization, staging and follow-up of treatment effects (*6*). Currently, the most important disadvantages of FDG imaging in the head and neck region are the limited availability of the method and accumulation of FDG in some benign salivary gland tumors (*27*) and inflammatory tissue (*28*). These limitations have to be weighed against the potential therapeutic gain associated with a better characterization of known cancer in a patient presenting with a head and neck tumor.

ACKNOWLEDGMENTS

REFERENCES

1. Adams GL. Treatment of head and neck cancer with combined modalities. *Invest Radiol* 1989;24:562–567.
2. Sturgis EM, Weiner RS, Miller RH. Laryngeal preservation. *J La State Med Soc* 1995;147:9–15.
3. Corvò R, Giaretti W, Sanguineti G, et al. Potential doubling time in head and neck tumors treated by primary radiotherapy: preliminary evidence for a prognostic significance in local control. *Int J Radiat Oncol Biol Phys* 1993;27:1165–1172.
4. Grandis JR, Tweardy DJ. Elevated levels of transforming growth factor α and epidermal growth factor receptor messenger RNA are early markers of carcinogenesis in head and neck cancer. *Cancer Res* 1993;53:3579–3584.
5. Klijanienko J, El-Naggar AK, de Braud F, et al. Tumor vascularization, mitotic index, histopathologic grade and DNA ploidy in the assessment of 114 head and neck squamous cell carcinomas. *Cancer* 1995;75:1649–1656.
6. Rege S, Maass A, Chaiken L, et al. Use of positron emission tomography with fluorodeoxyglucose in patients with extracranial head and neck cancers. *Cancer* 1994;73:3047–3058.
7. Braams JW, Pruim J, Freling NJM, et al. Detection of lymph node metastases of squamous-cell cancer of the head and neck with FDG-PET and MRI. *J Nucl Med* 1995;36:211–216.
8. McGuirt WF, Williams DW, Keyes JW, et al. A comparative diagnostic study of head and neck nodal metastases using positron emission tomography. *Laryngoscope* 1995;105:373–375.
9. Haberkorn U, Strauss L, Reisser Ch, et al. Glucose uptake, perfusion and cell proliferation in head and neck tumors: relation of positron emission tomography to flow cytometry. *J Nucl Med* 1991;32:1548–1555.
10. Di Chiro G. Positron emission tomography using [18F]fluorodeoxyglucose in brain tumors: a powerful diagnostic and prognostic tool. *Invest Radiol* 1986;22:360–371.
11. Griffeth LK, Dehdashti F, McGuire AH, et al. PET evaluation of soft tissue masses with fluorine-18 fluoro-2-deoxy-D-glucose. *Radiology* 1992;182:185–194.
12. Okada J, Yoshikawa K, Itami M, et al. Positron emission tomography using fluorine-18-fluorodeoxyglucose in malignant lymphoma: a comparison with proliferative activity. *J Nucl Med* 1992;33:325–329.
13. Hermanek P, Sobin LH, eds. *UICC TNM classification of malignant tumors*, 4th ed. Berlin: Springer-Verlag; 1992.
14. Rowell NP, McCready VR, Tait D, et al. Technetium-99m HMPAO and SPECT in the assessment of blood flow in human lung tumors. *Br J Cancer* 1989;59:135–141.
15. Hamacher K, Coenen HH, Stöcklin G. Efficient stereospecific synthesis of no-carrier-added 2-[18F]fluoro-2-deoxy-D-glucose using aminopolyether supported nucleophilic substitution. *J Nucl Med* 1986;27:235–238.
16. Minn H, Leskinen-Kallio S, Lindholm P, et al. Fluorine-18-fluorodeoxyglucose uptake in tumors: kinetic vs. steady-state methods with reference to plasma insulin. *J Comput Assist Tomog* 1993;17:115–123.
17. Zasadny K, Wahl RL. Standardized uptake values of normal tissues at PET with 2-[fluorine-18]-fluoro-2-deoxy-D-glucose: variations with body weight and a method for correction. *Radiology* 1993;189:847–850.
18. Minn H, Zasadny KR, Quint LE, Wahl RL. Lung cancer: reproducibility of quantitative measurements for evaluating 2-[F-18]-fluoro-2-deoxy-D-glucose uptake at PET. *Radiology* 1995;196:167–173.
19. Klemi P-J, Pylkkänen L, Kiilholma P, Kurvinen K, Joensuu H. p53 protein detected by immunohistochemistry as a prognostic factor in epithelial ovarian carcinoma. *Cancer* 1995;76:1201–1208.
20. Warburg O. On the origin of cancer cells. *Science* 1956;123:309–314.
21. Flier JS, Mueckler MM, Usher P, Lodish HF. Elevated levels of glucose transport and transport messenger RNA are induced by ras or src oncogenes. *Science* 1987;235:1492–1494.
22. Burk DM, Woods M, Hunter J. On the significance of glucolysis for cancer growth with special reference to Morris rat hepatomas. *J Natl Cancer Inst* 1967;38:839–863.
23. Tayek JA. A review of cancer cachexia and abnormal glucose metabolism in humans with cancer. *J Am Coll Nutr* 1992;11:445–456.
24. Minn H, Joensuu H, Ahonen A, Klemi P. Fluorodeoxyglucose imaging: a method to assess the proliferative activity of human cancer in vivo. *Cancer* 1988;61:1776–1781.
25. Kapoor RR, Spence AM, Muzi M, et al. Determination of the deoxyglucose and glucose phosphorylation ratio and the lumped constant in rat brain and a transplantable rat glioma. *J Neurochem* 1989;53:37–44.
26. Lapela M, Grénman R, Kurki T, et al. Head and neck cancer: detection of recurrence with positron emission tomography and 2-[fluorine-18]fluoro-2-deoxy-D-glucose. *Radiology* 1995;197:205–211.
27. Keyes JW Jr, Harkness BA, Greven KM, Williams DW, Watson NE, McGuirt WF. Salivary gland tumors: pretherapy evaluation with PET. *Radiology* 1994;192:99–102.
28. Kubota R, Yamada S, Kubota K, Ishiwata K, Tamahashi N, Ido T. Intratumoral distribution of fluorine-18-fluorodeoxyglucose in vivo: high accumulation in macrophages and granulation tissues studied by microautoradiography. *J Nucl Med* 1992;33:1972–1980.